Journal of Molecular Catalysis B: Enzymatic 66 (2010) 148–155

Contents lists available at ScienceDirect

Journal of Molecular Catalysis B: Enzymatic

journal homepage: www.elsevier.com/locate/molcatb

Functional characterization of a stereospecific diol dehydrogenase, FucO, from *Escherichia coli*: Substrate specificity, pH dependence, kinetic isotope effects and influence of solvent viscosity

Cecilia Blikstad, Mikael Widersten*

Department of Biochemistry and Organic Chemistry, Uppsala University, Box 576, SE-751 23 Uppsala, Sweden[1]

ARTICLE INFO

Article history:
Received 2 March 2010
Received in revised form 14 April 2010
Accepted 22 April 2010
Available online 15 May 2010

Keywords:
Diol dehydrogenase
Substrate specificity
Kinetic isotope effect
Kinetic mechanism

ABSTRACT

FucO, (*S*)-1,2-propanediol oxidoreductase, from *Escherichia coli* is involved in the anaerobic catabolic metabolism of L-fucose and L-rhamnose, catalyzing the interconversion of lactaldehyde to propanediol. The enzyme is specific for the *S*-enantiomers of the diol and aldehyde suggesting stereospecificity in catalysis. We have studied the enzyme kinetics of FucO with a spectrum of putative alcohol and aldehyde substrates to map the substrate specificity space. Additionally, for a more detailed analysis of the kinetic mechanism, pH dependence of catalysis, stereochemistry in hydride transfer, deuterium kinetic isotope effect of hydride transfer and effect of increasing solvent viscosity were also analyzed. The outcome of this study can be summarized as follows: FucO is highly stereospecific with the highest *E*-value measured to be 320 for the *S*-enantiomer of 1,2-propanediol. The enzyme is strictly regiospecific for oxidation of primary alcohols. The enzyme prefers short-chained (2–4 carbons) substrates and does not act on bulkier compounds such as phenyl-substituted alcohols. FucO is an 'A-side' dehydrogenase transferring the pro-*R*-hydrogen of NADH to the aldehyde substrate. The deuterium KIEs of k_{cat} and k_{cat}/K_M were 1.9 and 4.2, respectively, illustrating that hydride transfer is partially rate limiting but also that other reaction steps contribute to rate limitation of catalysis. Combining the KIE results with the observed effects of increasing medium viscosity proposed a working model for the kinetic mechanism involving slow, rate limiting, product release and on-pathway conformational changes in the enzyme–nucleotide complexes.

1. Introduction

The use of enzymes in organic synthesis is increasing and has been reported in reactions involving diverse chemistry [1–3]. The specificity of enzymes may relax the need for ultra-pure building blocks in organic synthesis allowing for enzymatically catalyzed reaction steps or enzymatic resolvation of racemic reactant mixtures that can be converted into optically pure products. The use of enzymes also contributes to sustainable approaches in the production of useful chemicals since aqueous solvents can be used and reactions may be run at moderate temperatures and pressures.

Propane-1,2-diol oxidoreductase (L-lactaldehyde reductase) belongs to the class III alcohol dehydrogenases, a class which is mainly populated by microbial enzymes, generally considered to be Fe(II)-dependent [4]. The *Escherichia coli* isoenzyme, FucO (encoded by the *fucO* gene), is one of the best studied family members and its metabolic role has been established [5]. FucO catalyzes the reduction of (*S*)-2-hydroxypropanal ((*S*)-lactaldehyde) by NADH (Scheme 1) in the anaerobic catabolism of L-fucose and L-rhamnose [5–10]. The enzyme also catalyzes the thermodynamically unfavored oxidation of (*S*)-1,2-propanediol into lactaldehyde using NAD^+ as cofactor [11]. FucO displays a strong preference for the *S*-isomer of 1,2-propanediol, suggesting stereospecificity in catalysis. The catalytic or kinetic mechanisms of FucO have not been extensively studied, however. A molecular model of a ternary complex of a coenzyme fragment and (*S*)-1,2-propanediol modeled into the active site (Fig. 1) [12] suggests a Lewis acid role for the iron cofactor thus stabilizing oxyanion reaction intermediates, similar to zinc-dependent alcohol dehydrogenases. Structural studies on other class III alcohol dehydrogenase enzymes support this proposal, although the role has not been experimentally verified [13–15]. The available crystal structures further indicate a restricted active site adapted to binding of short, unbranched aliphatic alcohols (Fig. 1B).

Due to the suggested stereospecificity, a primary purpose of the present work was to examine the functional properties of the FucO enzyme regarding substrate specificity and kinetic and catalytic mechanisms to assess its potential as biocatalyst for

* Corresponding author. Tel.: +46 (0) 18 471 4992; fax: +46 (0) 18 55 8431.
E-mail address: mikael.widersten@biorg.uu.se (M. Widersten).
[1] http://www.biorg.uu.se.

1381-1177/$ – see front matter © 2010 Elsevier B.V. All rights reserved.
doi:10.1016/j.molcatb.2010.04.010

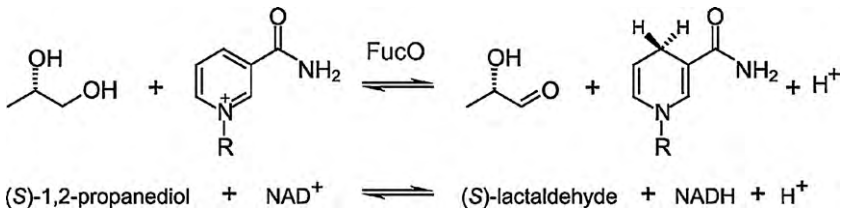

Scheme 1. Reversible FucO-catalyzed interconversion of (*S*)-1,2-propanediol to (*S*)-lactaldehyde using NAD^+/NADH as cofactors.

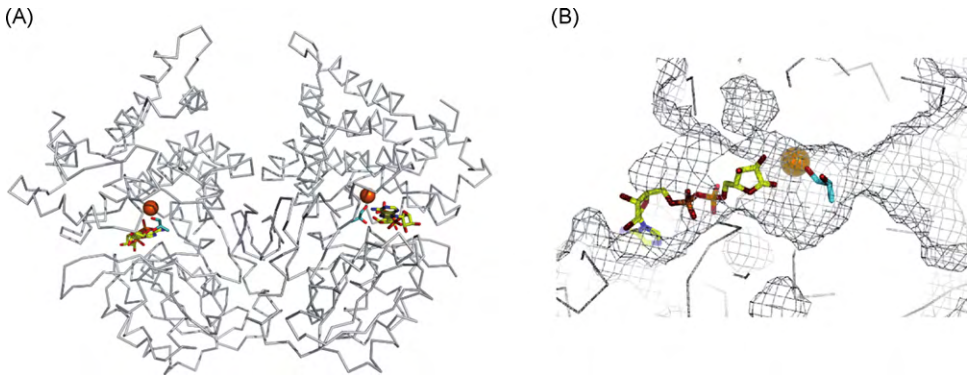

Fig. 1. Crystal structure of FucO from *E. coli*, in complex with adenosine-5-diphosphoribose, a Zn^{2+} ion (replacing in the crystal structure the native cofactor Fe^{2+}) and (*S*)-1,2-propanediol. (A) View of the native dimeric protein. (B) Close-up of the active site which is situated in a tunnel between two domains. The accessible volume of the active site is represented as a mesh. The NAD(H) analog adenosine-5-diphosphoribose is colored in yellow, the Zn^{2+} in orange and (*S*)-1,2-propanediol in cyan. Image was created from the atomic coordinates deposited as PDB entry 1RRM. (For interpretation of the references to color in this figure legend, the reader is referred to the web version of the article.)

stereospecific oxidation of vicinal diols. Furthermore, class III alcohol dehydrogenases are in comparison to the extensively studied class II isoenzymes (such as the liver and yeast alcohol dehydrogenases) relatively little studied. The present work thereby contributes to a further exploration of this enzyme family and also presents an opportunity to compare different classes of alcohol dehydrogenases. Substrate specificity has been evaluated by steady-state kinetics with a spectrum of candidate substrates (Fig. 2). Stereospecificity of the hydride transfer between cofactor and substrate has been determined using deuterated NADH and ^{1}H NMR. With the aim to describe kinetic and catalytic mechanisms including rate limiting reaction steps, we studied the enzyme kinetics during the steady state. The kinetic analyses were complemented by determinations of deuterium kinetic isotope effects (KIE) of hydride transfer, pH dependence of enzyme activity and influence of solvent viscosity on kinetic rates.

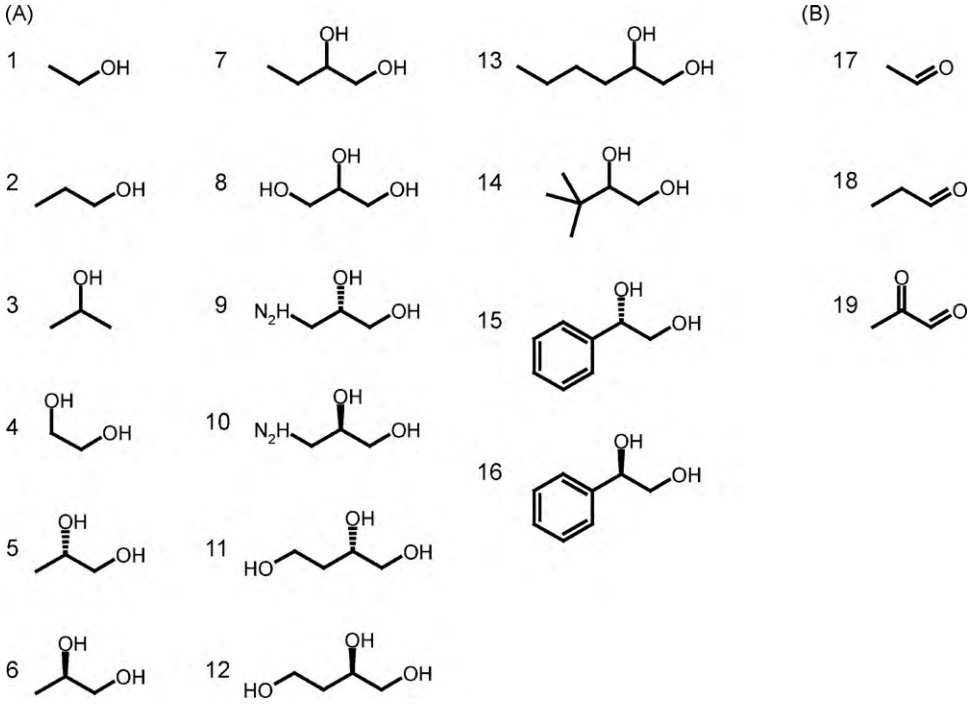

Fig. 2. Compounds tested as substrates for FucO, see Tables 1 and 2 for naming. (A) Alcohols and (B) aldehydes.

Table 1
Steady-state kinetic parameters for FucO-catalyzed alcohol oxidation at pH 10.0.

Substrate	k_{cat} (s^{-1})	K_M (mM)	k_{cat}/K_M (s^{-1} mM^{-1})	$E(S)/(R)$ (fold)
NAD^+	3.8 ± 0.1[a]	0.07 ± 0.01[a]	54 ± 2[a]	
Ethanol (1)	2.3 ± 0.06[b]	99 ± 4[b]	0.024 ± 0.0005[b]	
1-Propanol (2)	2.8 ± 0.05	12 ± 0.6	0.24 ± 0.008	
2-Propanol (3)	n.a.[c]	n.a.[c]	n.a.[c]	
1,2-Ethanediol (4)	4.0 ± 0.06	51 ± 2	0.08 ± 0.002	
(*s*)-1,2-Propanediol (5)	3.8 ± 0.04	5.4 ± 0.1	0.71 ± 0.01	320
(*r*)-1,2-Propanediol (6)	0.16 ± 0.01	74 ± 7	0.0022 ± 0.0001	
rac-1,2-Butanediol (7)	2.6 ± 0.05	6.9 ± 0.3	0.38 ± 0.01	
1,2,3-Propanetriol (8)	2.6 ± 0.07	140 ± 6	0.019 ± 0.0004	
(*S*)-3-Amino-1,2-propanediol (9)	0.88 ± 0.02	58 ± 2	0.015 ± 0.0004	170
(*R*)-3-Amino-1,2-propanediol (10)	–	–	0.00009 ± 0.00001	
(*S*)-1,2,4-Butanetriol (11)	1.9 ± 0.1	190 ± 20	0.010 ± 0.0003	20
(*R*)-1,2,4-Butanetriol (12)	0.22 ± 0.04	450 ± 90	0.0005 ± 0.00002	
rac-1,2-Hexanediol (13)	0.25 ± 0.003	13 ± 0.6	0.020 ± 0.0002	
rac-3,3-Dimethyl-1,2-butanediol (14)	–	–	0.00005 ± 0.00001	
(*S*)-1-Phenyl-1,2-ethanediol (15)	n.a.	n.a.	n.a.	
(*R*)-1-Phenyl-1,2-ethanediol (16)	n.a.	n.a.	n.a.	

[a] Determined in the presence of 15 mM (*S*)-1,2-propanediol.
[b] All alcohol oxidation reactions were determined in the presence of 0.2 mM NAD^+.
[c] n.a., no detectable enzyme activity.

2. Results and discussion

2.1. Gene cloning, heterologous expression and purification of FucO

An expression system producing C-terminally His-tagged FucO was constructed. The protein was expressed in *E. coli* and purified by Ni(II) affinity chromatography followed by a gel filtration step. As judged by Coomassie-stained SDS-PAGE the protein was homogeneous after the purification procedure. The extinction coefficient at 280 nm for the purified FucO protein was by quantitative amino acid analysis determined to be 41,000 M^{-1} cm^{-1}. The protein was purified with a typical yield of 0.3 μmol/l growth medium.

2.2. Catalytic function and substrate specificity

To achieve an overview of the substrate specificity profile of FucO, steady-state kinetic parameters were determined for both the oxidation and the reduction reactions with a set of alcohols and aldehydes (Fig. 2). The substrates displayed a variation in size, bulkiness, stereochemistry and position and number of substituents. The data are presented in Tables 1 and 2 and provide a basis for a structure profile of a FucO-accepted substrate:

(1) *Enantiopreference for diol substrates*: FucO is highly enantioselective with a 320-fold preference for (*S*)-1,2-propanediol as compared to the (*R*)-isomer. High degree of selectivity in favor of the *S*-enantiomers is also observed when tested for activity with compounds **9** and **10** or **11** and **12**.
(2) *Position of the oxidized hydroxyl group*: the enzyme displays strict regiospecificity, only reacting with primary alcohols. The catalyzed oxidation of 1-propanol proceeds with a relatively high catalytic efficiency of 0.24 s^{-1} mM^{-1} whereas 2-propanol is not converted at detectable levels.
(3) *Alkyl chain-length of accepted substrates:* A maximum catalytic efficiency is displayed with *n*-propyl- and *n*-butyl-substituted substrates. For the diols, the enzyme displays highest catalytic efficiencies with its natural substrate (*S*)-1,2-propanediol and *rac*-butanediol with k_{cat}/K_M values of 0.71 s^{-1} mM^{-1} and 0.38 s^{-1} mM^{-1}, respectively. For the shorter-chain substrate ethanediol, or the longer-chain substrate *rac*-hexanediol the efficiencies are considerably lower.
(4) *Substrate bulkiness*: Alcohols containing bulky substituents, e.g. compounds **14**–**16**, are not converted at detectable levels.

The reduction of aldehyde is the thermodynamically favored reaction which is reflected in the 40-fold higher k_{cat}/K_M for the catalyzed reduction of propanal as compared to the oxidation of 1-propanol, determined at optimal pH for either reactions. The higher catalytic efficiency is displayed in both k_{cat} and K_M and in addition, K_M is 3–4 fold lower for NADH than for NAD^+.

With respect to the purpose of evaluating the biocatalytic potential of FucO, the data shows that the enzyme is highly enantioselective and strictly regiospecific. Hence, FucO is a candidate biocatalyst for primary alcohol oxidation of (*S*)-diols generating stereopure α-hydroxyl substituted aldehydes, or reduction of the latter. The preference of FucO for low-molecular substrates, however, limits the scope of possible reactant alcohols and aldehydes that would be effectively converted by this enzyme. This limitation in substrate preference is in accordance with the tertiary structure of FucO [12] which reveals that the substrate binding site is restricted by a narrow waist and thereby adopting this enzyme for acting primarily on low-molecular substrates (Fig. 1B). However, this waist consists mainly of uncharged residues and is a potential target for expanding the substrate specificity through directed evolution.

Table 2
Steady-state kinetic parameters for FucO-catalyzed aldehyde reduction at pH 7.

Substrate	k_{cat} (s^{-1})	K_M (mM)	k_{cat}/K_M (s^{-1} mM^{-1})
NADH	15 ± 0.2[a]	0.02 ± 0.001[a]	970 ± 40[a]
Ethanal (17)	7.3 ± 0.2[b]	11 ± 1[b]	0.65 ± 0.04[b]
Propanal (18)	20 ± 0.4	2.1 ± 0.1	9.2 ± 0.8
2-Oxopropanal (19)	10 ± 0.2	4.1 ± 0.3	2.5 ± 0.1

[a] Determined in the presence of 10 mM propanal.
[b] All aldehyde reduction reactions were determined in the presence of 0.2 mM NADH.

2.3. Stereospecificity in hydride transfer

NAD(P)-dependent alcohol dehydrogenases are as a rule stereospecific in the hydride transfer reaction from and to the cofactor [16]. Transfer occurs either of the pro-*R*- or the pro-*S*-hydrogen (A-side and B-side, respectively) at the carbon-4 position on the nicotinamide ring. In order to study the stereospecificity of FucO-catalyzed hydride transfer deuterated *R*- and *S*-NADH ([4*R*-^{2}H]NADH and [4*S*-^{2}H]NADH) were synthesized. As judged

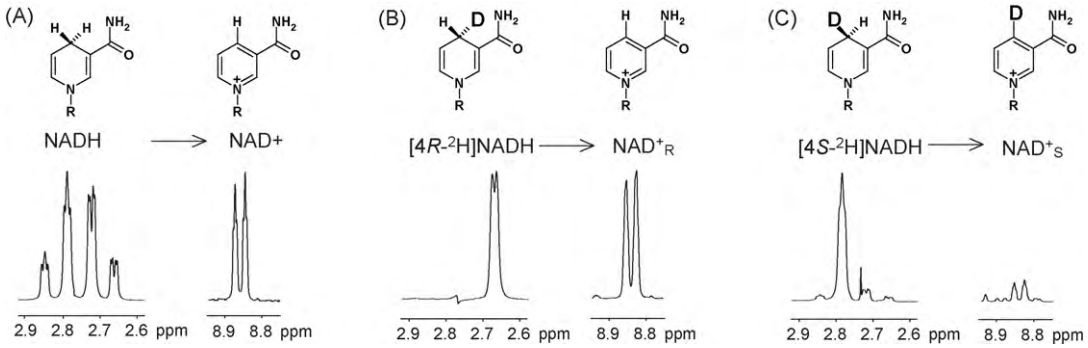

Fig. 3. ^{1}H NMR spectra showing the C-4 protons of the nicotinamide ring of (A) NADH and NAD$^+$, (B) [4*R*-^{2}H]NADH and NAD_R^+ and (C) [4*S*-^{2}H]NADH and NAD_S^+. In the spectrum of NAD_R^+ a peak correspond to the C4 proton of NAD$^+$. For NAD_S^+ no peak are detected at the same shift, the deuteron is retained on the NAD$^+$. Hence, the pro-*R*-hydrogen on NADH is transferred to the aldehyde substrate and the pro-*S*-hydrogen stays on NAD$^+$.

by ^{1}H NMR, the deuterated nucleotides were sufficiently pure and isotopic substitutions were at expected positions (Fig. 3). For [4*R*-^{2}H]NADH essentially complete replacement of hydrogen to deuterium had occurred (Fig. 3B). In [4*S*-^{2}H]NADH, traces of non-deuterated NADH were detected in the NMR spectra (Fig. 3C).

The produced [4*R*/*S*-^{2}H]NADH were enzymatically oxidized by FucO in the presence of propanal, producing NAD$^+$ (NAD_R^+ or NAD_S^+, respectively). The hydrogen of interest, the C-4 hydrogen of NAD$^+$, is shown as a doublet peak at 8.9 ppm in the ^{1}H NMR spectrum (Fig. 3A). The spectrum of NAD_R^+ displays a peak corresponding to this hydrogen, while NAD_S^+ retains its deuterium and do not display a peak in this position (Fig. 3B and C). Hence, similar to class II alcohol dehydrogenases, the *R*-hydrogen of NADH is being transferred by FucO, classifying the enzyme as an A-side dehydrogenase.

2.4. pH dependence of catalysis

pH dependence of k_{cat} and k_{cat}/K_M for the oxidation reaction was assayed with the natural substrate (*S*)-1,2-propanediol and with a model substrate, 1-propanol. For the reduction reaction the model substrate propanal was used. The enzyme displays highest oxidation efficiency at pH values around 10 with a 10-fold drop in activity at pH 9 and at pH 8 the enzyme is virtually inactive. The pH-dependencies of oxidation of both substrates are very similar and can be modeled by a single ionization event, with indistinguishable apparent $pK_a^{k_{cat}}$ values above 9 pH. Titrations of k_{cat}/K_M also appear to depend on single ionization events with apparent pK_a values of approximately 10 (Fig. 4, Table 3). The reduction reaction is more insensitive to changes in pH; k_{cat} and k_{cat}/K_M are virtually unchanged over a pH range from 5 to 9. However, pH values >9 result in decrease in enzyme activity (Fig. 4, Table 3).

The underlying mechanism of the strong pH dependence of the oxidation reaction is at present unclear and there is no obvious dependence on titratable groups in the expected catalytic mechanism. Side-chain functional groups of Lys ($-NH_3^+$), Tyr (–OH) or Cys (–SH) all display typical pK_a values in the range of 9–11 and investigation of the FucO active-site structure identifies only one candidate residue that may be involved in catalysis, Lys162. This residue is conserved among related primary structures such as group III alcohol dehydrogenases and in homologous putative enzymes, derived from deposited gene sequences. Lys162 contributes to the cofactor binding site [12,13] by forming a hydrogen bond with the 2′-hydroxyl group of the nicotinamide ribose and the side-chain ε-ammonium group. The local arrangement of hydrogen bond networks resembles somewhat the proton transfer chain that has been established in class II alcohol dehydrogenases with a proposed role of shuttling the hydroxyl proton from the substrate out of the active site to solvent during the oxidation reaction [17,18]. In the horse liver alcohol dehydrogenase, this proton is transferred from the alcohol via a Ser hydroxyl and the nicotinamide ribose 2′-hydroxyl to a surface-located His. A corresponding putative proton shuttle in FucO would begin at the primary hydroxyl group of the substrate via a water molecule to the nicotinamide ribose 2′-hydroxyl group, further to Lys162 and Asn71 and ending up at the surface-located Asn274. Consequently, the observed pH dependence could be due to that a deprotonated lysine would accelerate proton transfer, possibly enhancing the overall catalytic rate, as compared to a protonated lysine. Another explanation of the pH profile of the oxidation reactions could simply be due to the

Table 3
pH dependence of k_{cat} and k_{cat}/K_M.

Substrate	pK_a (k_{cat})	pK_a (k_{cat}/K_M)
(*S*)-1,2-Propanediol	9.4 ± 0.3	10.2 ± 0.4
1-Propanol	9.3 ± 0.6	10.1 ± 0.5
Propanal	>9.0	>9.5

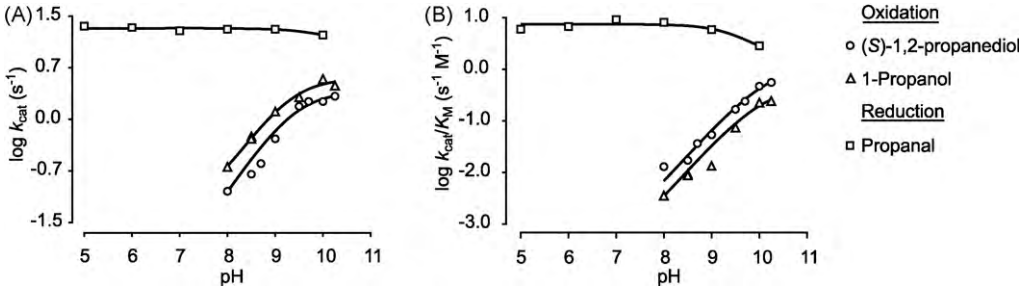

Fig. 4. The effect of pH of (A) k_{cat} and (B) k_{cat}/K_M of FucO-catalyzed reactions. The catalyzed oxidation of (*S*)-1,2-propanediol and 1-propanol display a strong pH dependence while reduction of propanal is relatively unaffected by pH. Solid lines represent the fits of Eq. (3) to the experimental data, and provide estimates of apparent pK_a values (Table 3).

$$E{\cdot}NAD^+ + R\text{-}OH \underset{k_{-1}}{\overset{k_1[R\text{-}OH]}{\rightleftharpoons}} E{\cdot}NAD^+{\cdot}R\text{-}OH \underset{k_{-2}}{\overset{k_2}{\rightleftharpoons}} E{\cdot}NADH{\cdot}R{=}O \xrightarrow{k_3} E{\cdot}NADH + R{=}O \xrightarrow{k_4} E + NADH$$

Scheme 2. Minimal mechanism of FucO-catalyzed alcohol oxidation under pseudo first-order conditions with saturating concentrations of NAD^+.

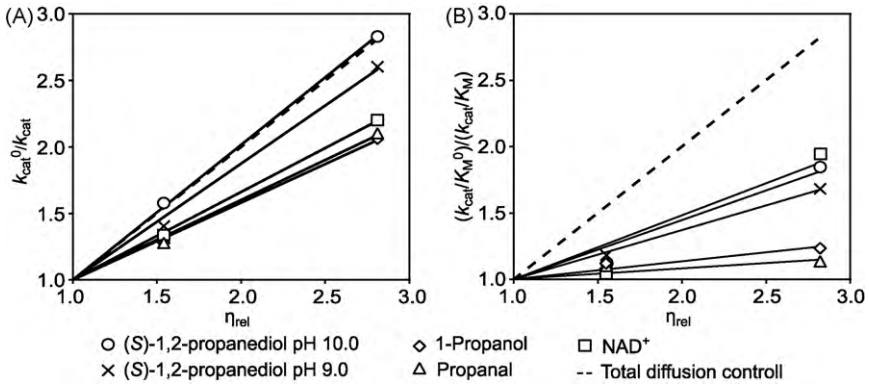

Fig. 5. Medium viscosity effect of k_{cat} for FucO-catalyzed reactions. Plot of (A) k_{cat}^0/k_{cat} and (B) $(k_{cat}/K_M^0)/(k_{cat}/K_M)$ vs. relative viscosity (η_{rel}) for oxidation of (*S*)-1,2-propanediol pH 10.0, (*S*)-1,2-propanediol pH 9.0, propanol and NAD^+ (with 1-propanol) and reduction of propanal in sucrose-containing buffer. Dashed line illustrates a completely diffusion-limited reaction (slope = 1).

increased hydroxide ion concentration facilitating alcohol deprotonation accompanied by a loss in enzyme activity at higher pH values due to denaturation of the tertiary structure.

2.5. Kinetic mechanism of FucO

To simplify the analysis of the results from the deuterium KIE and the solvent viscosity effects, a minimal kinetic mechanism of the FucO-catalyzed reaction has been applied. The simplified model is valid for measurement of initial rates under pseudo first-order conditions and in the presence of saturated concentrations of NAD^+. The model describes an ordered bi-bi mechanism with four steps (Scheme 2):

The model includes (I) reversible association/dissociation of substrate (R–OH) to the E–NAD^+ complex, with rates k_1 and k_{-1}. (II) Reversible deprotonation and hydride transfer, with rates k_2 and k_{-2}. (III and IV) Irreversible product release, dissociation of aldehyde (R=O), with rate k_3 and nucleotide (NADH) release, with rate k_4. The steady-state rate equation for this reaction results in expressions for k_{cat} (Eq. (1)) and k_{cat}/K_M (Eq. (2)).

$$k_{cat} = \frac{k_2 k_3}{k_2 + k_{-2} + k_3 + (k_2 k_3/k_4)} \quad (1)$$

$$\frac{k_{cat}}{K_M} = \frac{k_1 k_2 k_3}{k_{-1}(k_{-2} + k_3) + k_2 k_3} \quad (2)$$

From these expressions it can be concluded that reaction rates contributing to k_{cat} includes steps from the Michaelis complex to product release (k_2, k_{-2}, k_3 and k_4). Reaction rates contributing to k_{cat}/K_M includes steps for the initial binding of the alcohol up to and including the first irreversible step (k_1, k_{-1}, k_2 and k_{-2} and k_3).

2.5.1. Solvent viscosity effects on k_{cat} and k_{cat}/K_M

Kinetic rates dependent on diffusion are influenced by the viscosity of the solvent [19–23]. Hence, a decrease in catalytic rates with increased viscosity implies that diffusion-controlled steps such as association of substrate, dissociation of product and/or conformational changes required for catalysis are rate limiting. If the kinetic parameters k_{cat} or k_{cat}/K_M show dependencies on viscosity, the relative change in value (k_{cat}^0/k_{cat} or $(k_{cat}/K_M)^0/(k_{cat}/K_M)$, respectively) versus the relative medium viscosity (η_0/η) should follow a linear relationship. The magnitude of the slope reflects the degree of diffusion control where a unit slope indicates total diffusion limitation. In the minimal mechanism for FucO (Scheme 2) the chemical step is assumed to be independent of solvent viscosity. Steps related to substrate binding and aldehyde and nucleotide release are, if measured individually, assumed to be dependent on solvent viscosity. From relationships between k_{cat} and k_{cat}/K_M and individual rate constants in the kinetic mechanism it can be derived that: (1) The influence on k_{cat} (Eq. (1)) by solvent viscosity reflects the extent to which rates for product and nucleotide release (k_3 and k_4) limits the catalytic turnover. (2) The influence on k_{cat}/K_M (Eq. (2)) reflects the extent to which rates for substrate binding (k_1 and k_{-1}) and aldehyde release (k_3) limits the catalytic efficiency under sub-saturating conditions.

All studied FucO-catalyzed reactions displayed a decrease in k_{cat} with increased solvent viscosity proposing a diffusion-controlled rate limiting step involved in product release, k_3 and/or k_4 (Fig. 5, Table 4). The influence of viscosity on k_{cat} for the reaction with the most favored substrate, (*S*)-1,2-propanediol at pH 10.0, showed a linear dependency with a unit slope (slope = 1) suggesting a totally diffusion-controlled reaction dependent on product release. The reaction with the less favored substrate, 1-propanol, was to a lower degree affected by the increase of viscosity (slope = 0.6) showing that the rate of turnover for 1-propanol is both dependent on steps involving product release, and the chemical step. Indicating that product release is rate determining with the preferred substrate, while for the less favored substrate the hydride transfer also contributes to rate limitation.

The solvent viscosity effects on k_{cat}/K_M are qualitatively similar to the k_{cat} situation (Table 4, Fig. 5B). Association of enzyme and substrate are rarely rate limiting for k_{cat}/K_M, and in the present case where these values are modest (0.3–9 s^{-1} mM^{-1}; Tables 1 and 2), any effects due to lowered substrate association rates can safely

Table 4
Viscosity dependence of k_{cat} and k_{cat}/K_M.

Substrate	Slope k_{cat}^0/k_{cat}	Slope $k_{cat}/K_M^0/k_{cat}/K_M$
(*S*)-1,2-Propanediol, pH 10.0	1.0	0.5
(*S*)-1,2-Propanediol, pH 9.0	0.9	0.4
1-Propanol	0.6	0.1
Propanal	0.6	0.1
NAD^+	0.7	0.5

Table 5
Deuterium kinetic isotope effect of k_{cat} and k_{cat}/K_M.

Substrate	pH	k_{cat} (s^{-1})	k_{cat}/K_M (s^{-1} mM^{-1})	^{D}V	$^{D}V/K$
1-Propanol	9.0	1.5 ± 0.04	0.065 ± 0.005		
1,1-d_2-Propanol	9.0	0.77 ± 0.02	0.015 ± 0.0006	1.9 ± 0.07	4.3 ± 0.4
1-Propanol	10.0	4.3 ± 0.1	0.34 ± 0.02		
1,1-d_2-Propanol	10.0	2.3 ± 0.1	0.080 ± 0.005	1.9 ± 0.1	4.2 ± 0.4

be ruled out. Observed solvent viscosity effects on k_{cat}/K_M should therefore primarily be caused by product release. Further, since the expression describing k_{cat}/K_M (Eq. (2)) is independent of the rates of nucleotide release (k_4), any observed effect can be attributed to aldehyde or alcohol release, or possibly to potential rate limiting conformational changes. Hence, the overall lower viscosity effects on k_{cat}/K_M as compared to the effects on k_{cat} (Table 4) suggest that the primary cause for the observed decrease in turnover number at higher medium viscosities is primarily due to decreased nucleotide dissociation rates. Also, the fact that the viscosity effects on k_{cat} and on k_{cat}/K_M are of the same magnitude for the oxidation (1-propanol) and the reduction reactions (propanal), points towards that a diffusion-controlled step is rate limiting in both reaction directions.

2.5.2. Deuterium kinetic isotope effect

In the analysis of deuterium KIE on k_{cat} (^{D}V) and k_{cat}/K_M ($^{D}V/K$) any observed effects were treated as resulting from primary isotope effects, decreasing the rate of bond breaking and formation during hydride transfer from alcohol substrate to NAD^+ (Scheme 2). If this isotope-sensitive step was to be totally rate determining, the KIE of k_{cat} would represent the intrinsic isotope effect [24,25]. However, if hydride transfer is not solely rate determining the KIE will be masked by other kinetically slow steps preceding or succeeding the isotope-sensitive step. The observed KIE will then be described by ^{D}k, the intrinsic isotope effect on the forward rate constant for the isotopic-sensitive step, $^{D}K_{eq}$ the forward equilibrium isotope effect and c_f and c_r, the forward and reverse commitment factors, respectively. The commitment factors are composites of the relative values for rate constants for the isotope-sensitive step and flanking steps, and describe the tendency for the reaction to proceed in the forward or reverse directions from the hydride transfer step.

The deuterium KIEs measured for the oxidation of 1-propanol at pH 9.0 and 10.0 are shown in Table 5. The $^{D}V/K$ (4.2–4.3) is larger than ^{D}V (1.9) and both are independent of pH. The fact that there is a clear KIE demonstrates that hydride transfer is rate limiting. However, since the intrinsic KIE is unknown it cannot be established whether it is one of several rate limiting steps in the reaction or the sole rate determining one. Furthermore, the fact that $^{D}V/K$ is larger than ^{D}V suggests that steps contributing to k_{cat} and not to k_{cat}/K_M are slow in comparison with other steps and thus mask the KIE (see Scheme 2 and Eqs. (1) and (2)). By this it is given that the rate of the second half of the reaction (E·NAD^+·R–OH → E + NADH + R=O) must be slower than the first half (E·NAD^+ + R–OH → E·NADH + R=O). Consequently, reaction steps following the first irreversible step after catalysis, thus, steps involving nucleotide release are slower than steps involving substrate binding. Applying the method of Northrop [26] and assuming an upper limit of ^{D}k of 15 [26], one can calculate that the second half of the reaction ought to be 2.6–14.6 times slower than the first half.

An added uncertainty to the comparison of ^{D}V and $^{D}V/K$ is if a stabilized Michaelis complex at a sufficiently low energy level is present on the reaction path. This situation may cause an 'entrapment' of the Michaelis complex in an energetic pit resulting in a rate limiting energy barrier for product formation. This can give rise to a decrease in the KIE of k_{cat} but will not affect k_{cat}/K_M [24,25]. Since k_{cat}/K_M is the apparent 2nd order rate constant for free enzyme(-nucleotide complex) reacting with free alcohol to form aldehyde and NADH, this parameter will not be affected by a change in stabilization of the Michaelis complex and, hence, the magnitude of $^{D}V/K$ will be unaffected while ^{D}V will be decreased. In such a situation the values of the two parameters cannot be compared. On the other hand, if enzyme–substrate association/dissociation is in rapid equilibrium, the values of ^{D}V and $^{D}V/K$ may be used in comparison. In the present case, due to the high K_M of 1-propanol (12 mM), it is reasonable to assume that substrate binding is in rapid equilibrium and consequently the comparison of ^{D}V and $^{D}V/K$ would be valid.

2.5.3. Conformational change of enzyme–nucleotide complex

Steps in the catalytic mechanism for FucO which can be assumed to be affected by diffusion rates are the dissociation of product(s) and potential conformational changes of the enzyme or enzyme–substrate complexes. The combined results from KIE and solvent viscosity effects suggest that both hydride transfer and a conformational change of enzyme–nucleotide complex contribute to the rate limitation of oxidation of 1-propanol. Moreover, since the medium viscosity effects are higher for the more favored substrate (*S*)-1,2-propanediol, it is indicated that the rate limitation in this reaction is shifted towards the conformational change. Based on the observed deuterium KIEs we propose that this conformational change occur in the enzyme–nucleotide complex after the aldehyde product has been released but before nucleotide dissociation, thus affecting the rate of k_4.

Inspired by well characterized mechanisms in other alcohol dehydrogenases and experimental data from this study we propose an extended model of the kinetic mechanism of FucO-catalyzed alcohol oxidation as shown in Scheme 3.

The mechanism is, as the minimal one, an ordered bi-bi mechanism with NAD^+ binding first and release of aldehyde precedes that of NADH. Additionally, it involves a conformational change of the nucleotide-enzyme complex resulting in an altered enzyme form, E*. The change is believed to occur before alcohol binding; consequently a conformational change back to E occurs before release of the reduced nucleotide. Two different enzyme forms have likewise been invoked for a class II alcohol dehydrogenase, the horse liver alcohol dehydrogenase. In this enzyme, a diffusion-controlled association of enzyme and NAD^+ followed by a partially rate limiting conformational change forming a closed form of the enzyme–nucleotide complex [27], has been demonstrated. The conformational change occurring after chemical steps has also been suggested to be rate limiting [28].

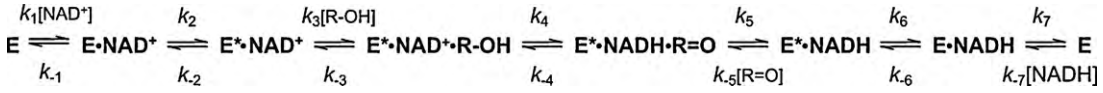

Scheme 3. Model for kinetic mechanism of FucO-catalyzed alcohol oxidation.

3. Conclusion

The class III alcohol dehydrogenases are in comparison to other alcohol dehydrogenases relatively little studied, therefore this report provides new insight into the kinetic and catalytic properties of this enzyme family and in particular the FucO enzyme from *E. coli*. The study has demonstrated FucO to be highly stereoselective and strictly regiospecific, exemplified by an *E*-value of more than 300 for the most selective enantiomers and solely reacting with primary alcohols. With respect to the catalytic and kinetic mechanisms we propose an ordered bi–bi mechanism involving a conformational change of the enzyme–substrate complex. Steps involving product release, possibly the proposed conformational change, are shown to be rate limiting for k_{cat}.

We are at present constructing enzyme-catalyzed synthesis pathways for the production of modular chemical substances, containing chiral centers and functional groups such as alcohols, aldehydes and ketones that are amenable to further derivatizations. The strategy relies on enzymes that catalyze specific reaction types and acts on a set of structurally related substrates in order to produce a spectrum of product molecules with controlled diversity. The high degree of selectivity makes FucO a potential enzyme for such applications. Additionally, enzyme engineering targeting the entrance to the substrate binding site constitutes a promising target for manipulation of substrate specificity, generating enzyme mutants amenable to accept a range of different diols and α-hydroxyl substituted aldehydes.

4. Experimental procedures

4.1. Chemical and reagents

All chiral and deuterated chemicals were purchases from Sigma-Aldrich. Purity of chiral substrate were: (*S*)/(*R*)-1,2-propanediol; ≥99%, (*S*)/(*R*)-3-amino-1,2-propanediol; 98%, (*S*)/(*R*)-1,2,4-butanetriol; ≥95%/98%, (*S*)/(*R*)-1-phenyl-1,2-ethanediol; 99%/98%. Degree of heavy isotope of deuterated reagents were: 1-1-d_2-propanol; 98 atom% D, ethanol-d_5; 99.5 atom% D, glucose-1-*d*; 98 atom% D. Enzymes used in synthesis of deuterated NADH were purchased from Sigma–Aldrich; glucose-6-phosphate dehydrogenase from *Leuconostoc mesenteroides*, ammonium sulphate suspension, 4.6 mg protein/ml, 715 units/mg protein. Alcohol dehydrogenase from bakers yeast, crystallized and lyophilized, ∼90% protein and <2% citrate buffer, 451 units/mg solid, 507 units/mg protein.

4.2. Gene cloning, heterologous expression and purification of FucO

The coding region of *fucO* from *E. coli* was amplified from genomic DNA of strain XL1-Blue (Stratagene) by PCR using forward primer: 5′-TTT TTT CTC GAG ATG ATG GCT AAC AGA ATG ATT-3′, and reverse primer: 5′-TTT TTT TCT AGA TTA TTA ACT AGT CCA GGC GGT ATG GTA AAG-3′. One bacterial colony was added to the reaction mixture in a volume of 50 μl and subjected to PCR. The PCR product was subcloned between the *Xho*I and *Spe*I sites of pGTacStEH1-5H [29] resulting in the pGTacfucO-5H expression plasmid. The subcloned gene fragment was sequenced in full to confirm sequence integrity, after which pGTacfucO-5H was transformed into *E. coli* XL1-Blue for protein production. Expression and purification of the C-terminally 5-His-tagged FucO enzyme was performed essentially according to a previously described procedure used for *Solanum tuberosum* epoxide hydrolase [29], with the exception that 100 μM of $FeCl_2$ was added together with the transcription inducer IPTG.

4.3. Catalytic function and substrate specificity

Steady-state kinetics was measured spectrophotometrically by monitoring the initial reaction velocities of the enzymatic activity. The reaction was followed by measuring the change in concentration of NADH at 340 nm ($\Delta\varepsilon = 6.22\ mM^{-1}\ cm^{-1}$). All steady-state measurements were performed at 30 °C using a Shimadzu UV-1700 spectrophotometer. The kinetic parameters, k_{cat}, K_M and k_{cat}/K_M, were determined under pseudo first-order conditions with a set of various alcohols and aldehydes (Fig. 2) in the presence of saturating concentration, 0.2 mM, of respective cofactor and varied concentration of alcohol or aldehyde. Kinetic parameters for the nucleotides were determined in the presence of 15 mM (*S*)-1,2-propanediol or 10 mM propanal together with varying concentration of NAD^+ or NADH, respectively. Oxidation reactions were performed in 0.1 M glycine–NaOH, pH 10.0, and reduction reactions in 0.1 M sodium phosphate, pH 7.0. Kinetic parameters were extracted by fitting the Michaelis–Menten equation using non-linear regression to the experimental data using MMFIT and RFFIT in SIMFIT (http://www.simfit.man.ac.uk/).

4.4. Stereospecificity of hydride transfer

[4*R*-^{2}H]NADH (A-side NADD) was synthesized and purified according to a revised protocol of Hallis and Liu [30]. 860 units yeast alcohol dehydrogenase, 0.14 mmol NAD^+ and 8.5 mmol ethanol-d_5 (added in portions of 1.7 mmol every 20 min) were mixed in 15 ml 50 mM NH_4HCO_3 and incubated at room temperature for 1.5 h. [4*S*-^{2}H]NADH (B-side NADD) was synthesized according to a revised protocol of Viola et al. [31]. 200 units glucose-6-phosphate dehydrogenase, 0.18 mmol NAD^+ and 0.20 mmol glucose-d_1 was mixed in 9 ml 50 mM NH_4HCO_3 and 3 ml dimethyl sulphoxide, and incubated at room temperature for 24 h. The reactions were followed by the increase in absorbance at 340 nm. At equilibrium, protein was removed by ultrafiltration. Subsequently, the nucleotides were purified by anion exchange chromatography on a 16 mm × 70 mm column (Fractogel® EMD TMAE (M), Merck) pre-equilibrated with H_2O. Reaction mixture was applied to the column, at a flow rate of 1 ml/min, and unreacted substrate was washed off by 75 ml H_2O followed by 30 ml of 50 mM NH_4HCO_3 at a flow rate of 3 ml/min. Nucleotides was subsequently eluted with 200 mM NH_4HCO_3 at a flow rate of 1 ml/min. Nucleotide containing fractions were pooled and the nucleotide were lyophilized. Purity and isotopic incorporation of deuterium was analyzed by ^{1}H NMR using a Varian 300 (for ^{1}H NMR spectrum of NADH see [32]).

0.015 mmol of prepared [4*R*/*S*-^{2}H]NADH, 0.15 mmol propanal, added in portions of 0.05 mmol every 30 min, and 0.015 μmol of purified FucO was incubated in 5 ml 50 mM NH_4HCO_3. After 1.5 h at room temperature the reaction had reached equilibrium. Protein was removed by ultrafiltration and the remaining reaction mixture was lyophilized. The presence of deuterium or hydrogen at position C-4 in the produced NAD^+ was analyzed by ^{1}H NMR (for ^{1}H NMR spectrum of NAD^+ see [33]).

4.5. pH dependence of catalysis

pH dependence of FucO catalysis was investigated by determining steady-state kinetics of the oxidation and reductions reactions, respectively. Measurements were conducted as described in Section 4.3. Catalytic function and substrate specificity. For alcohol oxidation, enzyme activity with (*S*)-1,2-propanediol and 1-propanol, in the presence of saturating concentrations of NAD^+, were measured at pH values ranging from 8.0 to 10.25. For aldehyde reduction, activity was determined in the presence of NADH and varying concentrations of propanal at pH vales ranging from 5.0 to 10.0. Buffers used were: 0.1 M sodium phosphate, pH 5.0–8.5,

0.1 M glycine–NaOH, pH 8.5–10.25. Apparent pK_a values for k_{cat} and k_{cat}/K_M were determined by fitting Eq. (3), describing dependence of activity of a single ionization using RFFIT. L_H is the titrated parameter of k_{cat} and k_{cat}/K_M, and L_{HA} and L_A are the amplitude factors for the protonated or deprotonated enzyme forms, respectively.

$$L_H = \frac{L_{HA}[H^+] + L_{A^-} + K_a}{K_a + [H^+]} \quad (3)$$

4.6. Solvent viscosity effects on k_{cat} and k_{cat}/K_M

Steady-state kinetics for (*S*)-1,2-propanediol, 1-propanol, NAD^+ (30 mM 1-propanol used as second substrate) and propanal was performed in buffers of various viscosities. Experiments were conducted as described in Section 4.3. Catalytic function and substrate specificity, but with 0–30% (w/v) of sucrose included as a microviscogen. Relative viscosities (η_{rel}) of the buffers in 30 °C were determined for 15% sucrose to 1.5 and for 30% sucrose to 2.8 using an Ubbelohde viscometer. The relative change in values for k_{cat} and k_{cat}/K_M were plotted versus the η_{rel} and the slope represents the magnitude of solvent viscosity dependence.

4.7. Deuterium kinetic isotope effects

The deuterium kinetic isotope effect of k_{cat} and k_{cat}/K_M for 1-propanol and 1-1-d_2-propanol was determined at pH values 9.0 and 10.0. Measurements were performed in the presence of saturating concentrations of NAD^+ as described in Section 4.3. Catalytic function and substrate specificity. The deuterium kinetic isotope effect on k_{cat}, ^DV, was calculated from the ratio of $k_{cat}{}^H/k_{cat}^D$ [25]. The deuterium kinetic isotope effect on k_{cat}/K_M, $^DV/K$, was determined accordingly.

Acknowledgments

We thank A. Gogoll, from our department for valuable advice during NMR analyses. This work was supported by The Swedish Research Council and The Carl Trygger Foundation. C. Blikstad is a Lawski Foundation stipendiate.

References

[1] V.B. Urlacher, R.D. Schmid, Curr. Opin. Chem. Biol. 10 (2006) 156–161.
[2] S. Matsumura, Y. Soeda, K. Toshima, Appl. Microbiol. Biotechnol. 70 (2006) 12–20.
[3] E. García-Urdiales, I. Alfonso, V. Gotor, Chem. Rev. 105 (2005) 313–354.
[4] M.F. Reid, C.A. Fewson, Crit. Rev. Microbiol. 20 (1994) 13–56.
[5] L. Baldomá, J. Aguilar, J. Bacteriol. 170 (1988) 416–421.
[6] J. Ros, J. Aguilar, Biochem. J. 231 (1985) 145–149.
[7] J. Badia, J. Ros, J. Aguilar, J. Bacteriol. 161 (1985) 435–437.
[8] E.H. Patel, L.V. Paul, S. Patrick, V.R. Abratt, Res. Microbiol. 159 (2008) 678–684.
[9] S. Sridhara, T.T. Wu, T.M. Chused, E.C. Lin, J. Bacteriol. 98 (1969) 87–95.
[10] G.T. Cocks, T. Aguilar, E.C. Lin, J. Bacteriol. 118 (1974) 83–88.
[11] A. Boronat, J. Aguilar, J. Bacteriol. 140 (1979) 320–326.
[12] C. Montella, L. Bellsolell, R. Pérez-Luque, J. Badía, L. Baldoma, M. Coll, J. Aguilar, J. Bacteriol. 187 (2005) 4957–4966.
[13] D. Marçal, A.T. Rêgo, M.A. Carrondo, F.J. Enguita, J. Bacteriol. 191 (2009) 1143–1151.
[14] S.N. Ruzheinikov, J. Burke, S. Sedelnikova, P.J. Baker, R. Taylor, P.A. Bullough, N.M. Muir, M.G. Gore, D.W. Rice, Structure 9 (2001) 789–802.
[15] R. Schwarzenbacher, F. von Delft, J.M. Canaves, L.S. Brinen, X. Dai, A.M. Deacon, M.A. Elsliger, S. Eshaghi, R. Floyd, A. Godzik, C. Grittini, S.K. Grzechnik, C. Guda, L. Jaroszewski, C. Karlak, H.E. Klock, E. Koesema, J.S. Kovarik, A. Kreusch, P. Kuhn, S.A. Lesley, D. McMullan, T.M. McPhillips, M.A. Miller, M.D. Miller, A. Morse, K. Moy, J. Ouyang, R. Page, A. Robb, K. Rodrigues, T.L. Selby, G. Spraggon, R.C. Stevens, H. van den Bedem, J. Velasquez, J. Vincent, X. Wang, B. West, G. Wolf, K.O. Hodgson, J. Wooley, I.A. Wilson, Proteins 54 (2004) 174–177.
[16] H.F. Fisher, E.E. Conn, B. Vennesland, F.H. Westheimer, J. Biol. Chem. 202 (1953) 687–697.
[17] T. Ehrig, T.D. Hurley, H.J. Edenberg, W.F. Bosron, Biochemistry 30 (1991) 1062–1068.
[18] H. Eklund, B.V. Plapp, J.P. Samama, C.I. Brändén, J. Biol. Chem. 257 (1982) 14349–14358.
[19] A.C. Brouwer, J.F. Kirsch, Biochemistry 21 (1982) 1302–1307.
[20] B.M. Wood, K.K. Chan, T.L. Amyes, J.P. Richard, J.A. Gerlt, Biochemistry 48 (2009) 5510–5517.
[21] M. Toth, J. Zajicek, C. Kim, C.W. Chow, C. Smith, S. Mobashery, S. Vakulenko, Biochemistry 46 (2007) 5570–5578.
[22] B.E. Eser, P.F. Fitzpatrick, Biochemistry 49 (2010) 645–652.
[23] C.B. Grissom, W.W. Cleland, Biochemistry 27 (1988) 2927–2934.
[24] P.F. Cook, W.W. Cleland, Biochemistry 20 (1981) 1790–1796.
[25] D.B. Northrop, Annu. Rev. Biochem. 50 (1981) 103–131.
[26] D.B. Northrop, Biochemistry 14 (1975) 2644–2651.
[27] V.C. Sekhar, B.V. Plapp, Biochemistry 29 (1990) 4289–4295.
[28] M.J. Hardman, Biochem. J. 195 (1981) 773–774.
[29] L.T. Elfström, M. Widersten, Biochem. J. 290 (2005) 633–640.
[30] T.M. Hallis, H. Liu, Tetrahedron 54 (1998) 15975–15982.
[31] R.E. Viola, P.F. Cook, W.W. Cleland, Anal. Biochem. 96 (1979) 334–340.
[32] X. Yang, S. Bi, L. Yang, Y. Zhu, X. Wang, Spectrochim. Acta 59 (2003) 2561–2569.
[33] X. Yang, S. Bi, X. Yang, L. Yang, J. Hu, J. Liu, Z. Yang, Anal. Sci. 19 (2003) 815–821.